Planetary and Space Science 60 (2012) 199–206

Contents lists available at SciVerse ScienceDirect

Planetary and Space Science

journal homepage: www.elsevier.com/locate/pss

Surface age of the ice–dust mantle deposit in Malea Planum, Mars

Malte Willmes [a,*], Dennis Reiss [a,1], Harald Hiesinger [a,1], Michael Zanetti [b,2]

[a] Institut für Planetologie, Westfälische Wilhelms-Universität Münster, Wilhelm-Klemm-Straße 10, 48149 Münster, Germany
[b] Department of Earth and Planetary Science, Washington University, St. Louis, Campus Box 1169, One Brookings Drive, St. Louis, MO 63130, USA

ARTICLE INFO

Article history:
Received 17 February 2011
Received in revised form
1 July 2011
Accepted 19 August 2011
Available online 26 August 2011

Keywords:
Mars
Malea Planum
Ice–dust mantle
Crater degradation
Recent martian climate change

ABSTRACT

The mid- and high-latitudes of Mars are covered by a smooth young mantle that is interpreted as an atmospherically derived air-fall deposit of ice and dust related to recent climate changes. In order to determine relative and absolute ages of this surface unit within the southern hemisphere, a systematic survey of all available HiRISE and CTX images in the Malea Planum region from 55–60°S latitude and 50–70°E longitude was performed and the distribution and the morphology of small impact craters on the mantle deposit were investigated. Using crater size-frequency measurements, we derived absolute model ages of ~3–5 Ma for the surface of the mantle, immediately south of the Hellas basin rim. Morphologic observations of the mantle, its fresh appearance, very low number of craters, and superposition on older units support this very young Amazonian age. Nearly all observed craters on the smooth mantle in Malea Planum are small and show signs of erosion, evidence for the ongoing modification of the ice–dust mantle. However, this modification has not been strong enough to reset the surface age. Compared to the ice–dust mantle at higher latitudes in the northern and southern hemisphere, the surface of the mantle in Malea Planum is older and thus has been relatively stable during obliquity changes in the last ~3–5 Ma. This is consistent with the hypothesis that the ice–dust mantle is a complex surface deposit of different layers, that shows a strong latitude dependence in morphology and has been deposited and degraded at different times in martian history.

1. Introduction

1.1. The ice–dust mantle and the Martian climate

The mid- and high-latitudes of Mars are covered by a young, layered ice–dust mantle that varies in thickness and is usually independent of local geology, topography, and elevation (Mustard et al., 2001). In particular, the mantle at high latitudes ($>60^\circ$) is continuous and extensively covered by patterned ground, except where it is interrupted by polar cap outliers, dunes, or steep slopes. However, the uppermost meters of this mantle occur in patches that are surrounded by degraded terrain, which exposes deeper layers of the mantle (e.g., Schon et al., 2009). At mid-latitudes, from 30°–60°, the ice–dust mantle shows extensive signs of erosion, and is referred to as dissected mantle terrain (Mustard et al., 2001). Milliken and Mustard (2003) characterized three different erosional styles that range from localized complete removal, which is most extensive at lowest latitudes, to knobby and wavy dissection and scalloped terrain at higher latitudes (Milliken and Mustard, 2003). The knobby and wavy dissection is characterized by areas of smooth intact mantle adjacent to areas of incomplete removal of the mantle. The scalloped terrain is not spatially extensive but concentrated in certain areas, like Utopia Planitia in the northern hemisphere and Malea Planum in the southern hemisphere, and is characterized by the degradation of large portions of the mantle (e.g., Lefort et al., 2010; Zanetti et al., 2010). The latitudes below $\pm 30^\circ$ of Mars are essentially unmantled (Milliken and Mustard, 2003). Different distribution and emplacement mechanisms have been proposed for the ice–dust mantle (e.g., Mellon and Jakosky, 1995; Head et al., 2003; Mellon et al., 2004, 2008). Investigations by Schon et al. (2009) indicate that among the proposed models, the atmospheric deposition of ice and dust during obliquity excursions is most consistent with the observed data.

Unlike Earth, Mars has experienced dramatic shifts in obliquity during its geologic history. Models of the obliquity for the last 10 Ma are well constrained (Laskar et al., 2004), and can be used for precise palaeoclimate studies (Mischna et al., 2003; Levrard et al., 2004; Forget et al., 2006; Schorghofer, 2007). The models show that ~5 Ma ago, Mars moved from a phase of high mean obliquity ($\sim 35 \pm 10^\circ$) to lower mean obliquity ($\sim 25 \pm 10^\circ$). This resulted in the migration of H_2O to the poles from low- and mid-latitude ice

* Corresponding author. Tel. +49 251 83 39047.
E-mail addresses: ifp@uni-muenster.de, Malte.willmes@uni-muenster.de (M. Willmes), Michael.Zanetti@wustl.edu (M. Zanetti).
[1] Tel.: +49 251 83 33496; fax: +49 251 83 36301.
[2] Tel.: +1 314 935 5610.

0032-0633/$ - see front matter © 2011 Elsevier Ltd. All rights reserved.
doi:10.1016/j.pss.2011.08.006

deposits (Levrard et al., 2004). Despite lower mean obliquity in the recent past, Mars still experienced numerous short duration cycles of higher obliquity values ($>30^{\circ}$) during the last 5 Ma (Laskar et al., 2002, 2004). During these phases the insolation on the polar region increases and water vapor is released, leading to the deposition of a mixture of ice and dust in the mid- and high-latitudes in both hemispheres (Head et al., 2003; Mischna et al., 2003; Levrard et al., 2004; Forget et al., 2006). This is a rapid process and a period of $\sim$40 ka is considered to be long enough to deposit a meter thick ice–dust mantle (Head et al., 2003). During phases of lower obliquity, the water–ice in the lower latitudes becomes unstable, sublimes back into the atmosphere, and retreats to the poles. Pure ice mantles can come and go without leaving any trace. However if ice is mixed with dust, a protective lag deposit can form and the further degradation of the mantle is then controlled by the stability of ground ice (Mellon and Jakosky, 1995; Schorghofer and Aharonson, 2005; Mellon et al., 2004; Schorghofer, 2007). Thus a protective lag deposit allows patches of the ice–dust mantle to exist at latitudes where near-surface ice is unstable under current obliquity conditions (Byrne et al., 2009).

The obliquity cycles of Mars thus lead to the repeated emplacement and degradation of layers of the ice–dust mantle over million year time scales (Mustard et al., 2001; Kreslavsky and Head, 2002; Head et al., 2003; Kostama et al., 2006). The ice–dust mantle is older than the last obliquity excursion 0.4–2.1 Ma ago (Head et al., 2003; Kreslavsky and Head, 2002) and it consists of different layers that form a complex surface deposit (Mustard et al., 2001; Kreslavsky and Head, 2002; Kostama et al., 2006; Schon et al., 2009). Under current obliquity conditions ($\sim$25°) ground ice is unstable at latitudes below $\sim$50° (Mellon et al., 2004; Schorghofer and Aharonson, 2005), leading to the extensive removal and degradation of the ice–dust mantle in the low- and mid-latitudes in both hemispheres if the protective lag deposit is removed.

1.2. Geologic context of Malea Planum

The study region is located at 55–60°S latitude and 50–70°E longitude and encompasses the northern highlands of Malea Planum, a large, flat, volcanic plain located at the southern rim of the Hellas basin (Fig. 1). It is part of the Circum-Hellas Volcanic Province (Greeley et al., 2007; Williams et al., 2009, 2010) and consists of several volcanic units of late Noachian and Hesperian age, including the major volcanic structures Peneus, Malea, Pityusa, and Amphitrites Paterae (Tanaka et al., 2002; Plescia, 2003; Williams et al., 2009, 2010). Amphitrites Patera and Peneus Patera are both interpreted to consist of pyroclastic material (Tanaka and Leonard, 1995; Williams et al., 2008). Amphitrites is a low relief shield whereas Peneus does not show a clear shield structure (Tanaka and Leonard, 1995; Williams et al., 2008). Both paterae are surrounded by the ridged plains in the south and the channels of Axius Valles in the north (Tanaka and Leonard, 1995).

A dominant feature at the southern margin of the study region is Barnard crater, a central ring impact crater about 130 km in diameter. The topographically highest features in the study region are parts of the crater rim of Barnard crater ($\sim$2.2 km) and the rim of Amphitrites Patera ($\sim$1.9 km). North of Amphitrites Patera the terrain slopes towards Hellas at about 1.2–1.5° and wrinkle ridges with a relief of several hundred meters extend across the plains in radial patterns around the paterae (Tanaka and Leonard, 1995; Plescia, 2003, 2004; Williams et al., 2008). Shield-like deposits around the patera at the northern edges of Malea Planum have been observed by Greeley and Guest (1987). These deposits have scarps and ridges trending toward Hellas Planitia, interpreted to be the result of the modification of low viscosity lava flows by fluvial channeling (Greeley and Guest, 1987).

1.3. The ice–dust mantle in Malea Planum

Under present atmospheric conditions the mantle in Malea Planum is undergoing degradation when the protective lag deposit is removed (e.g., Lefort et al., 2010; Zanetti et al., 2010). From Gamma Ray Spectrometer measurements (GRS) $\sim$6 to $\geq$20 wt% water ice are within a meter of the surface (Feldman et al, 2002, 2004) and ice stability models (Boynton et al., 2002; Mellon et al., 2004; Chamberlain and Boynton, 2007) predict ground ice to be stable in the shallow subsurface below depths of $\sim$10s of centimeters. In addition, martian climate models suggest that high concentrations of ice are found at greater depth (Levrard et al., 2004). In Malea Planum the ice–dust mantle is draped over the local topography throughout the study region and is interpreted to consist of continuous smooth patches and degraded terrain (Fig. 2). Zanetti et al. (2010) found that in places the surface of the mantle shows a texture similar to the basketball terrain, which has been described in the northern hemisphere above 60° (Malin and Edgett, 2001; Kreslavsky and Head, 2002;

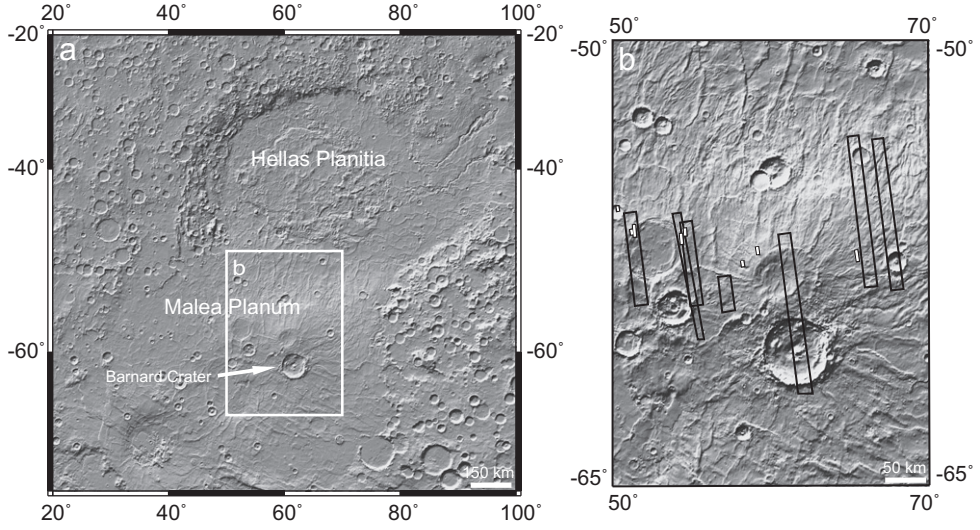

Fig. 1. (a) MOLA shaded relief map of Hellas Planitia and Malea Planum on Mars. White box shows the location of the study area. (b) Close up of the study region including the image footprints for HiRISE (solid white boxes) and CTX (black boxes).

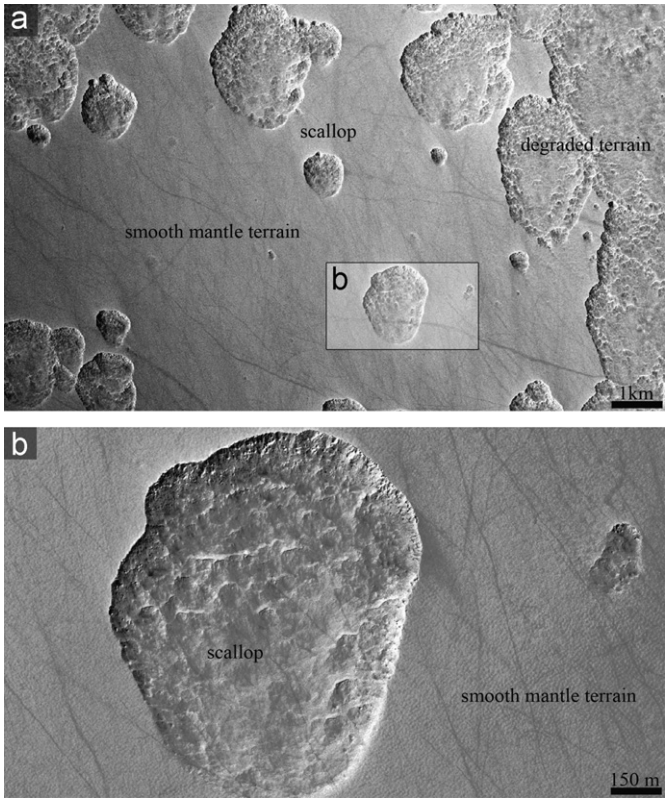

Fig. 2. Smooth mantle and degradation features at (a) CTX and at (b) HiRISE resolution. The uppermost part of the mantle forms a smooth terrain and shows a clear boundary to the degraded terrain. Only the smooth terrain was mapped, excluding the degraded and scalloped terrain from our measurements. The dark streaks in the image are dust devil tracks. North is up in both images (CTX image: P08_004274_1221; HiRISE image: ESP_014005_1225).

Head et al., 2003). In addition, features interpreted to be small sublimation polygons and/or thermal contraction cracks, as well as scalloped terrain, which in the southern hemisphere is concentrated in Malea Planum, have been observed (Marchant and Head, 2007; Zanetti et al., 2010). Scallops exhibit an N–S asymmetric profile with a steep pole-facing scarp, and a gentle equator-facing slope. Their shape ranges from highly elongated to almost circular. They are rimless and shallow and are tens of meters to a few kilometers large (Milliken and Mustard, 2003; Morgenstern et al., 2007; Lefort et al., 2010; Soare et al., 2007; Zanetti et al., 2010). Scalloped depressions are thought to form in areas with thick mantle deposits when ice from the ice–dust mantle sublimes (Milliken and Mustard, 2003; Plescia, 2003; Morgenstern et al., 2007; Zanetti et al., 2010). Scallop formation is suggested to start from small cracks, which presumably form due to thermal contraction of the depositional mantle (Morgenstern et al., 2007; Lefort et al., 2010; Zanetti et al., 2010). In this scenario asymmetrical depressions form during periods of low to moderate obliquity ($<30^{\circ}$), which then grow retrogressively in equatorward direction during phases of high obliquity ($>40^{\circ}$), by the destabilization of the pole-facing slope (Lefort et al., 2009, 2010; Ulrich et al., 2010). Scallop growth thus requires obliquity variations, the presence of subsurface ground-ice, and a removal process for the protective lag deposit. This removal can be achieved, for example, by dust devils, strong slope winds related to the Hellas basin, and/or the formation of small impact craters (Siili et al., 1999; Mustard et al., 2001; Zanetti et al., 2010). Scallops are found within continuous patches of the smooth mantle and they can coalesce to form large irregularly-shaped scalloped terrain (Milliken and Mustard, 2003; Lefort et al., 2010; Zanetti et al., 2010).

The thickness of the ice–dust mantle in Malea Planum varies considerably. A distinct boundary, where mantle thickness increases coincides with the onset of the slope of the Hellas basin north of $\sim$58°S (Zanetti et al., 2010). Thick deposits that cover larger topographic features are found close to the rim of the Hellas basin. While the plains of Malea Planum are covered by a thinner mantle, isolated thick patches of mantle terrain occur south of $\sim$58°S. Quantitative estimates by Zanetti et al. (2010) using crater diameter/rim height geometry ratios and depth measurements of scallops revealed that the mantle is at least 5 m thicker at the wall of the Hellas basin than on the highlands of Malea Planum. Thick deposits of the ice–dust mantle often completely cover any given crater, leading to an underestimation of the thickness (Zanetti et al., 2010). Depth measurements of the scallops using individual MOLA points indicate an average depth of 10–20 m. Since the observed scallops do not erode the entire mantle, but excavate a deeper layer of the ice–dust mantle; this value is also considered a minimum estimate (Zanetti et al., 2010). The average thickness of the mantle deposit in our study region is estimated to be $\sim$25 m (Zanetti et al., 2010). In this paper, we combine morphologic observations with our newly derived absolute model surface ages to constrain the modification of the ice–dust mantle in Malea Planum and relate it to other ice–dust mantle deposits in the northern and southern hemisphere.

2. Methods

2.1. Image data

We investigated all available Context Camera (CTX, $\sim$5 m/pxl) (Malin et al., 2007) and High Resolution Imaging Science Experiment (HiRISE, $\sim$0.25–0.5 m/pxl) (McEwen et al., 2007) images as released until January 2011 of the Malea Planum region. We focused our analysis on the images that contain large, homogeneously appearing, patches of smooth mantle (>5 km^2), not considering areas of degraded and heavily scalloped terrain (Table 1). The smooth mantle unit was mapped and its area was calculated using ESRI ArcGIS^{TM} software. All primary craters on the smooth mantle unit were measured with the Cratertools plug-in for ESRI ArcGIS^{TM} (Kneissl et al., in press). The crater counts were imported into Craterstats (Michael and Neukum, 2010) in which model ages were calculated using the production function of Neukum et al. (2001) and the chronology function of Hartmann and Neukum (2001). The crater morphologies were investigated using HiRISE images and compared to the different classes of crater degradation on the ice–dust mantle described by Maine et al. (2010).

2.2. Crater size frequency distributions and model ages

Crater size-frequency distribution measurements are a well established technique to determine relative and absolute surface ages using remote sensing images. Relative ages can be determined on the basis of stratigraphic relationships, state of erosion and frequency and size of impact craters (e.g., Hartmann, 1973; Hartmann and Neukum, 2001; Hartmann, 2005). The crater production function for the Moon is well constrained and chronology models have been developed for the Moon on the basis of the Apollo sample radiometric ages. Using scaling laws these models were adapted for Mars (e.g., Hartmann and Neukum, 2001; Ivanov, 2001; Neukum et al., 2001). To derive absolute model ages for the smooth mantle unit in Malea Planum we fitted the production function (Ivanov, 2001; Neukum et al., 2001) to

Table 1
Summary of parameters for each individual HiRISE and CTX images used in this study.

Image identification	Center latitude [°]	Center longitude, E [°]	Image resolution [cm/pxl]	Smooth mantle area [km^2]	# Craters [Ø > 50 m]	Crater density [Ø > 50 m/km^2]
HiRISE						
PSP_003232_1220	−57.7	59.2	49.7	60.86	6	0.099
PSP_004168_1220	−57.9	65.5	24.9	69.22	3	0.043
PSP_004340_1235	−56.2	50.2	25.2	6.44	0	0.000
PSP_005421_1215	−58.1	58.2	25.2	16.99	1	0.059
PSP_005632_1225	−57.3	54.3	51.4	26.51	4	0.151
PSP_005698_1225	−57.0	51.3	26.8	33.81	0	0.000
ESP_013952_1225	−57.1	54.5	24.9	23.38	4	0.171
ESP_014005_1225	−57.1	51.1	26.7	41.35	2	0.048
				∑ 278.57	**∑ 20**	**0.071**
CTX						
P04_002731_1209	−59.19	57.21	500	38.49	1	0.026
P08_004274_1221	−58.01	51.46	501	253.66	6	0.024
P13_006212_1202	−59.83	61.51	503	1121.68	15	0.013
P16_007227_1236	−56.43	67.35	501	3340.04	37	0.011
P16_007438_1238	−56.34	65.75	498	3774.85	127	0.034
B04_011328_1215	−58.56	54.55	499	192.36	34	0.177
B07_012462_1219	−58.18	54.98	499	101.50	19	0.187
				∑ 8822.57	**∑ 239**	**0.067**

the measured crater size-frequency distribution of the measured surface unit and used the chronology model of Hartmann and Neukum (2001) and Ivanov (2001). While generally considered robust, there are several sources that introduce errors to our absolute model ages: (i) The scaling of crater diameters for impacts of the same-sized projectiles on the Moon and other planetary bodies, which is dependent, for example, on gravity, impact velocities, and target strengths (Ivanov, 2001). Ivanov (2001) calculated that compared to the Moon, the impact crater number on Mars does not differ more than ±50% from the crater number in the same diameter bin. The more frequent asteroid impacts on Mars do not result in a significantly higher cratering rate because the higher gravity and lower impact velocities result in smaller crater sizes on Mars. Ivanov (2001) found that the cratering rate Mars/Moon ratio is of the order of 0.6–1.2, depending on the steepness of the N(D) distribution. Hartmann and Neukum (2001) discussed several factors influencing the repeatability and accuracy of crater counts on Mars and concluded that ages can be determined with an accuracy of about 5–20%, not counting the uncertainties in the crater production rate on Mars relative to the Moon. The present day impact cratering rate on Mars has been estimated by Malin et al. (2006) using Mars Orbiter Camera (MOC) images and by Daubar et al. (2010) using CTX and HiRISE images. They are in excellent agreement with the production function of Hartmann and Neukum (2001). (ii) The influence of the martian atmosphere on the formation of small craters is difficult to assess and could introduce errors in the absolute surface age particularly for small craters (e.g., Chappelow and Sharpton, 2005). (iii) The role of secondary impact craters for age determinations on terrestrial planets has been discussed in detail (e.g., McEwen and Bierhaus, 2006). Hartmann et al. (2008) and Werner et al. (2009) demonstrated that the assumption that most of the small impact craters on Mars are secondary craters is not supported by the observed data. Using reasonable predictions of the crater size-frequency distribution of secondary craters for a key case (Cerberus plains, Mars), Werner et al. (2009) showed that the effect of secondary impact cratering on the model crater retention age is less than the statistical uncertainty. This is especially true for young surfaces that started to accumulate craters long after the large impacts that created distal secondary craters (Kreslavsky, 2009). Clusters of small craters, otherwise considered as clear indicators of secondary cratering, can also form by the atmospheric break-up of small meteoroids (Ivanov et al., 2008, 2009). In our analyses, we paid particular attention to avoid areas showing any signs of secondary craters, thus further minimizing this source of error, and note that there are no recent large impact craters, which might be a source for secondary projectiles.

3. The ice–dust mantle and crater size-frequency measurements

3.1. Morphologic observations

In order to investigate the development of the ice–dust mantle in Malea Planum, we combined morphologic observations of the mantle itself and its superposed impact craters with crater size-frequency measurements. The mantle in Malea Planum appears to be unusually thick (~25 m) for mid-latitudes and shows a high abundance of scalloped terrain (Lefort et al., 2010; Zanetti et al., 2010). Its thickness is most likely related to its position at the southern rim of the Hellas basin. The regional smooth slope and the local atmospheric conditions could have provided a favorable place to accumulate a thick mantle deposit (Zanetti et al., 2010). Alternatively, it is also plausible that the mantle has been preferentially preserved in this region (Zanetti et al., 2010).

Scallops are abundant in Malea Planum and their formation in this region might be related to the effective removal of the protective lag deposit by dust devils and strong slope winds that are related to the Hellas basin (Zanetti et al., 2010). In some areas the scalloped depressions coalesce to form large areas of degraded terrain. The area within this degraded terrain lacks impact craters, hindering the determination of reliable age estimations using crater statistics for these interstitial regions. The lack of impact craters is partially due to the fact that craters were removed during the erosional process that formed the degraded terrain. The formation of the scalloped terrain in Malea Planum either occurred during obliquity cycles within the last 5 Ma (Zanetti et al., 2010) or could be related to obliquity variations in the last 10 Ma (Ulrich et al., 2010). Since it was not possible to further constrain the timing of scallop formation in Malea Planum, no information about the timing of the emplacement and modification of the ice–dust mantle can be inferred from these features.

3.2. Crater degradation

Craters on the smooth ice–dust mantle undergo rapid erosion related to the modification of the ice–dust mantle (e.g., Banks et al., 2010; Maine et al., 2010). Maine et al. (2010) distinguished three different classes of impact craters: (i) newly formed craters that show bright exposed water ice, a raised rim, and an ejecta blanket, (ii) relatively fresh bowl-shaped craters that exhibit a strong topography and a sharp break in slope, and (iii) craters that have a shallow topography and are not strictly bowl-shaped. These classes form a continuous sequence of crater degradation that can be observed in high-resolution HiRISE images. The different stages of crater degradation observed in Malea Planum are shown in Fig. 3. In our study area we did not identify any fresh craters (class 1) and no ejecta blankets were observed. At the latitudes of our study area, this is expected as exposed ice is unstable and will quickly sublime (Dundas and Byrne, 2010). Young impact craters on Mars are often associated with rays that are typically dark (e.g., Malin et al., 2006; Golombek et al., 2010). However, the absence of crater rays is not conclusive as the production of rays is heavily dependent on local geology (e.g., Malin et al., 2006; Golombek et al., 2010). We identified only 8 craters with raised rims. The other observed craters on the ice–dust mantle are all degraded to some extent (class 2 and 3). The fast erosion of craters shows that the mantle undergoes degradation where the protective lag deposit is removed. The main processes of crater modification on the ice–dust mantle are accumulation of ice and dust, the sublimation of ice, mass wasting, and aeolian processes (e.g., Banks et al., 2010). After impact, the insolation on the crater walls leads to the sublimation of ice and the accumulation of lag deposits that eventually slump down into the crater. This infill and softening of the crater occurs over a longer timescale than ejecta obliteration, but still quickly in geologic terms (Banks et al., 2010). In addition, craters can also be traps for eolian deposits. Another process of crater degradation is the subsequent deposition of ice and dust that fills the crater. The detection of these smooth craters can be subjective, as it depends on illumination conditions, image quality, and other competing features such as small scallops. In some cases craters are not filled, but have initiated the erosion of the surrounding ice–dust mantle. Since scalloped depressions can begin to form once the protective dust cover of the ice–dust mantle has been removed, it is possible that the erosion of small craters can lead to the formation of scallops (Zanetti et al., 2010). We observed several scallops that looked similar to circular impact craters and are located within extensive patches of otherwise still intact mantle (Fig. 3).

3.3. Crater size-frequency measurements

Patches of the smooth upper mantle unit with a total area of 8823 km^2 in CTX and 280 km^2 in HiRISE were mapped, excluding all areas of degraded and scalloped terrain (Fig. 2). Some HiRISE images are located within CTX images leading to an overlap of

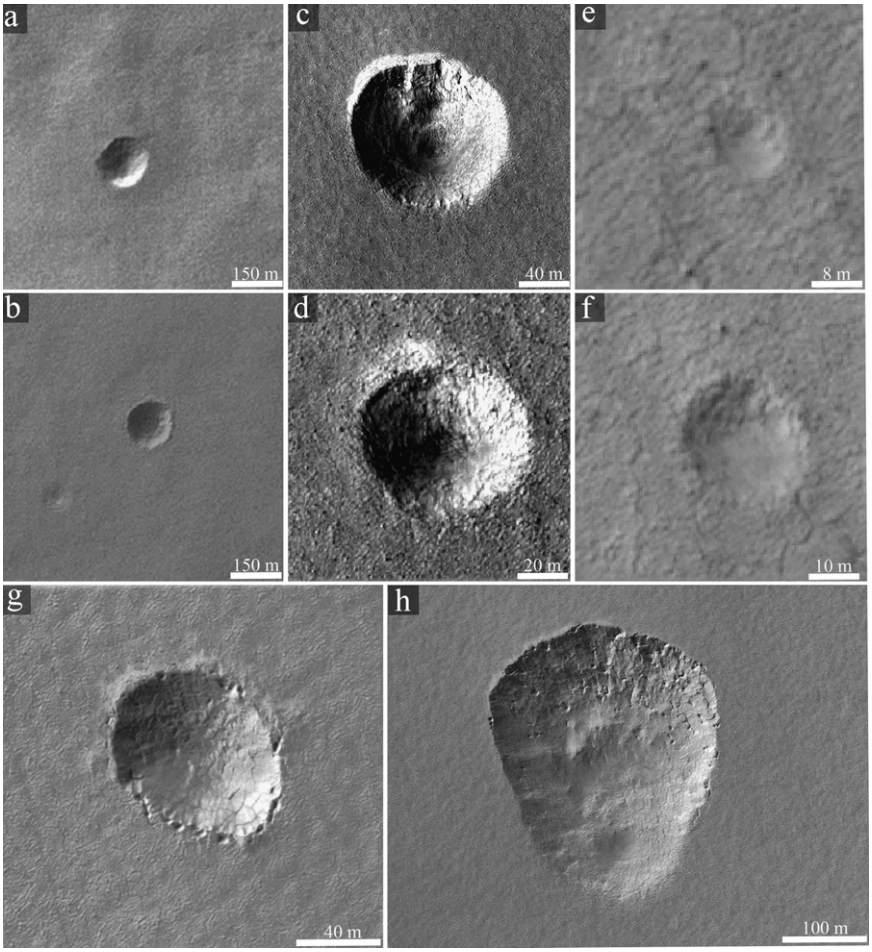

Fig. 3. Crater morphologies on the ice–dust mantle, north is up in all images; (a, b) relatively fresh craters at CTX resolution (P08_004274_1221). (c, d) Relatively fresh craters at HiRISE resolution (PSP_003232_1220). (e, f) Small degraded craters at HiRISE resolution (ESP_013952_1225). (g) Degraded crater past the point of secure identification forming a scallop-like feature (PSP_005632_1225). (h) Typical scalloped depression found in the study region (PSP_005632_1225) as a comparison for the degraded crater in image (g).

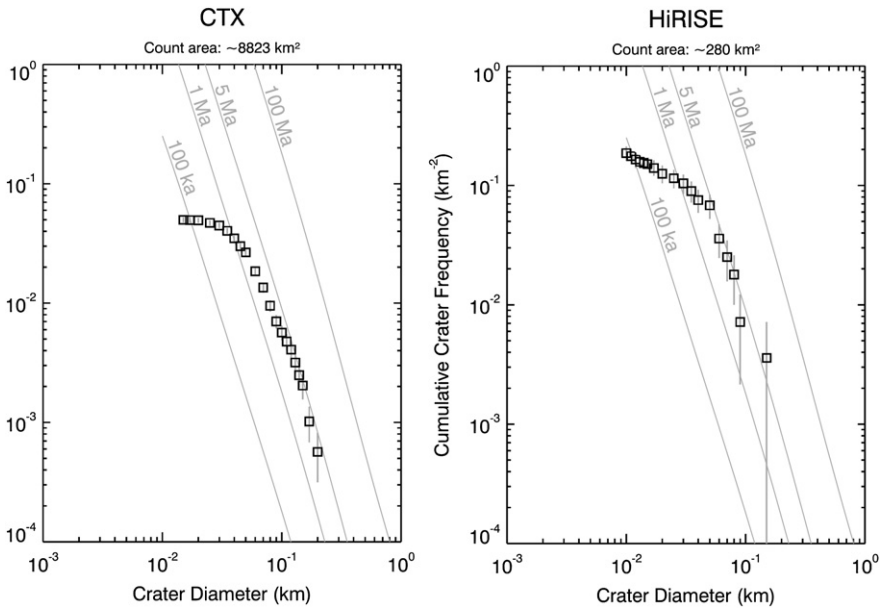

Fig. 4. Crater size-frequency measurements for the smooth mantle, obtained from CTX and HiRISE images.

$\sim$90 km^2. We were able to observe craters as small as $\sim$5 m (using HiRISE images with maximum resolution 0.25 m/pxl). Craters smaller than $\sim$5 m cannot confidently be distinguished from small-scale erosional features of the ice–dust mantle even in HiRISE images in our study region. The density of craters $>$50 m in diameter varies throughout the different images from 0.011 to 0.187 km^{-2} (Table 1). The average crater density is 0.071 km^{-2} for the HiRISE images and 0.067 km^{-2} for the CTX images. No latitudinal trend in age has been observed within the study region. Only three small clusters of impact craters were observed, potentially secondary craters, and were excluded from further analysis. Using the crater statistics we determined a crater retention age of $\sim$3–5 Ma for the uppermost part of the ice–dust mantle in Malea Planum (Fig. 4). The crater size-frequency measurements for both CTX and HiRISE produced the same model ages. The erosion of small craters is also observed in the crater count plots. In CTX and HiRISE the crater curve bends to the left at crater diameters of $\sim$50 m, indicating a lack of craters below that size, despite the fact that the image resolution is good enough to detect even smaller craters. Using crater depth/diameter ratios of 0.2 (Melosh, 1989; Strom et al., 1992), the depth of a crater with a diameter 50 m is roughly estimated to be $\sim$10 m. The loss of craters of this size on the ice–dust mantle is either related to the ongoing degradation of the mantle since its emplacement at least $\sim$3–5 Ma ago and/or to phases of deposition of the ice–dust mantle thick enough to obscure craters with diameters smaller than 50 m in diameter during the most recent obliquity excursions 0.4 and 2.1 Ma.

4. Discussion

4.1. Surface age interpretation

The present extent of the ice–dust mantle on Mars is the result of repeated episodes of deposition and degradation (Kreslavsky and Head, 2002; Head et al., 2003). Thus, our derived crater retention age is either connected to (i) the deposition of the mantle in Malea Planum, and/or (ii) to the degradation of an already present ice–dust mantle in Malea Planum that ceased $\sim$3–5 Ma ago and was extensive enough to completely reset the surface age. The high mean obliquity of Mars ($\sim 35 \pm 10^\circ$) before $\sim$5 Ma caused the ice–dust mantle to be stable in low- and mid-latitudes (e.g., Head et al., 2003; Levrard et al., 2004; Forget et al., 2006). Despite the lower mean obliquity since $\sim$5 Ma, Mars experienced numerous short duration cycles of higher obliquity values ($>30^\circ$), that led to the deposition of the ice–dust mantle in the mid- and high-latitudes (e.g., Head et al., 2003; Levrard et al., 2004; Forget et al., 2006). In this context, our derived surface age is more likely connected to the abundant deposition of the ice–dust mantle in Malea Planum $\sim$3–5 Ma ago, than to a wide spread degradation event before that time. The smooth and homogenous surface of the ice–dust mantle also points towards a deposition event. However, based on our crater retention ages and morphologic observations it is not possible to exclude the degradation scenario. An additional problem when interpreting the development of the ice–dust mantle is that no information can be inferred about its extent and thickness before the last emplacement. This means, that it is not possible to determine if the ice–dust mantle has been deposited on the bedrock or on an already present older ice–dust mantle deposit.

4.2. The ice–dust mantle in Malea Planum in a global context

The occurrence of the ice–dust mantle in the 30–55° latitude bands in both hemispheres has been related to the most recent depositional phases 0.4–2 Ma ago (Head et al., 2003). Above 60° the mantle is widely covered by polygonal patterns, which have been interpreted as sublimation polygons and/or thermal contraction cracks and are not found at lower latitudes (Head et al., 2003; Milliken and Mustard, 2003; Mangold, 2005; Kostama et al., 2006; Mellon, et al., 2008). This patterned ground is similar in both hemispheres despite the very different underlying local geology (Kreslavsky et al., 2010). A latitudinal trend for the surface age of the ice–dust mantle in the northern lowlands from young ages at high latitudes to older ages at lower latitudes has been proposed by Kostama et al. (2006), based on the spatial distribution of small craters and the mantle texture. They derived a mean crater retention age of $\sim$0.1 Ma for latitudes $>50^\circ$N, but also found several images for latitudes $<70^\circ$N that show a higher crater retention age of $\sim$2 Ma.

The modeled surface ages of ~3–5 Ma and morphologic observations of the ice–dust mantle in Malea Planum (55–60°S) suggest that the mantle in this region has been relatively stable during the last obliquity excursions, which affected the mid- and high-latitudes in both hemispheres. Since ~3–5 Ma, modification of the ice–dust mantle has occurred, but only the uppermost few meters of the mantle have been affected leading to the erosion of craters < 50 m in diameter. In addition to the degradation of the mantle, the loss of craters can also be related to the deposition of the ice–dust mantle 0.4 and 2 Ma ago (Head et al., 2003). Even more recent erosion of small fresh craters has been observed by Kreslavsky et al. (2010). Based on small fresh craters ($5\text{ m} < D < 50\text{ m}$) they derived a surface age of the ice–dust mantle of ~10–40 ka for the high-latitudes in the southern hemisphere (60–70°S). They found that the relative density of fresh craters in the northern hemisphere is at least an order of magnitude lower than in the southern hemisphere and attribute this difference to the deposition of the ice–dust mantle for high latitudes in response to the change of season of the perihelion. Fresh craters in the north were obliterated by the deposition ~1 ka ago, and in the south ~20 ka ago when the perihelion season was reversed (Kreslavsky et al., 2010). The same process might also have contributed to the obliteration of small fresh craters in our study region in Malea Planum.

5. Conclusions

Using crater size-frequency distribution measurements we derived an absolute model surface age of ~3–5 Ma for the ice–dust mantle in Malea Planum. The interpretation of this surface age is complicated by the fact that the ice–dust mantle on Mars has a complex geologic history, reflecting different phases of emplacement and degradation. Based on our morphologic observations and stability models of the ice–dust mantle during that time frame, the derived surface age is more likely related to the last major depositional phase than to a wide spread degradation event. Since ~3–5 Ma periods of mantle deposition and degradation have affected the upper meters of the mantle deposit in the study region, obliterating small craters < 50 m in diameter and partially eroding larger craters. This loss of craters on the ice–dust mantle is either related to the ongoing degradation of the mantle since its emplacement and/or to phases of deposition of the ice–dust mantle thick enough to obscure small craters during the most recent obliquity excursions 0.4 and 2.1 Ma ago. In comparison to the ice–dust mantle in other regions at mid- and high-latitudes on Mars, which have been heavily influenced by these most recent obliquity excursions, the mantle in Malea Planum has been relatively stable and retained its surface age.

Acknowledgments

Thanks go to the CTX and HiRISE teams for providing excellent image data to the scientific community. In addition we thank Veli-Petri Kostama and an anonymous reviewer for their constructive feedback that greatly improved this manuscript. This research has been partly supported by the Helmholtz Association through the research alliance 'Planetary Evolution and Life'.

References

Banks, M.E., Byrne, S., Galla, K., McEwen, A.S., Bray, V.J., Dundas, C.M., Fishbaugh, K.E., Herkenhoff, K.E., Murray, B.C., 2010. Crater population and resurfacing of the martian north polar layered deposits. Journal of Geophysical Research 115, E08006. doi:10.1029/2009JE003523.

Boynton, W.V., et al., 2002. Distribution of hydrogen in the near surface of Mars: evidence for subsurface ice deposits. Science 297, 81–85. doi:10.1126/science.1073722.

Byrne, S., et al., 2009. Distribution of mid-latitude ground ice on mars from new impact craters. Science 325, 1674. doi:10.1126/science.1175307.

Chamberlain, M.A., Boynton, W.V., 2007. Response of Martian ground ice to orbit induced climate change. Journal of Geophysical Research. 112, E06009. doi:10.1029/2006JE002801.

Chappelow, J.E., Sharpton, V.L., 2005. Influences of atmospheric variations on Mars's record of small craters. Icarus 178, 40–55. doi:10.1016/j.icarus.2005.03.010.

Daubar, I.J., McEwen, A.S., Byrne, S., Dundas, C.M., Kennedy, M., Ivanov, B.A., 2010. The current martian cratering rate. Lunar and Planetary Science Conference XXXXI #1978.

Dundas, C.M., Byrne, S., 2010. Modeling sublimation of ice exposed by new impacts in the martian mid-latitudes. Icarus 206, 716–728. doi:10.1016/j.icarus.2009.09.007.

Feldman, W.C., et al., 2002. Global distribution of neutrons from Mars: results from Mars Odyssey. Science 297, 75–78. doi:10.1126/science.1073541.

Feldman, W.C., Prettyman, T.H., Maurice, S., Plaut, J.J., Bish, D.L., Vaniman, D.T., Mellon, M.T., Metzger, A.E., Squyres, S.W., Karunatillake, S., Boyton, W.V., Elphic, R.C., Funsten, H.O., Lawrence, D.J., Tokar, R.L., 2004. Global distribution of near-surface hydrogen on Mars. Journal of Geophysical Research 109, E09006. doi:10.1029/2003JE002160.

Forget, F., Haberle, R.M., Montmessin, F., Levrard, B., Head, J.W., 2006. Formation of glaciers on Mars by atmospheric precipitation at high obliquity. Science 311 (5759), 368–371. doi:10.1126/science.1120335.

Golombek, M., Robinson, K., McEwen, A.S., Bridges, N., Ivanov, B., Tornabene, L., Sullivan, R., 2010. Constraints on ripple migration at meridiani planum from observations of fresh craters by opportunity and HiRISE. Liquid Propulsion Systems Centre XXXXI #2373.

Greeley, R., Guest, J.E., 1987. Geologic map of the eastern equatorial region of Mars. U.S. Geology Survey. Misc. Invest. Ser. Map I-1802B, scale 1:15,000,000.

Greeley, R., Williams, D.A., Fergason, R.L., Kuzmin, R.O., Raitala, J., Neukum, G., Baratoux, D., Pinet, P., Xiao, L., the HRSC Team, 2007. The Tyrrhena-Malea Volcanic Province, Mars.in: European Mars Science and Exploration Conference, Noordwijk, The Netherlands, 12–16 November 2007. Abstract, vol. 1118874, p. 244.

Hartmann, W.K., 1973. Martian cratering 4: mariner 9 initial analysis of cratering chronology. Journal of Geophysical Research 78, 4096–4116. doi:10.1029/JB078i020p04096.

Hartmann, W.K., 2005. Martian cratering 8: isochron refinement and the chronology of Mars. Icarus 174, 294–320. doi:10.1016/j.icarus.2004.11.023.

Hartmann, W.K., Neukum, G., 2001. Cratering chronology and the evolution of Mars. Space Science Reviews 96, 165–194.

Hartmann, W.K., Neukum, G., Werner, S., 2008. Confirmation and utilization of the "production function" size-frequency distributions of Martian impact craters. Geophysical Research Letters 35, L02205. doi:10.1029/2007GL031557.

Head, J.W., Mustard, J.F., Kreslavsky, M.A., Milliken, R.E., Marchant, D.R., 2003. Recent ice ages on Mars. Nature 426, 797–802. doi:10.1038/nature02114.

Ivanov, B.A., 2001. Mars/Moon cratering rate ratio estimates. Space Science Reviews 96, 87–104. doi:10.1029/JB078i020p04096 Journal of Geophysical Research, 78, 4096–4116.

Ivanov, B.A., Melosh, H.J., McEwen, A.S., HiRISE Team, 2008. Small Impact Crater Clusters in High Resolution HiRISE Images. Lunar and Planetary Science Conference XXXIX #1221.

Ivanov, B.A., Melosh, H.J., McEwen, A.S., HiRISE Team, 2009. Small Impact Crater Clusters in High Resolution HiRISE Images–II. Lunar and Planetary Science Conference XXXX #1410.

Kneissl T., van Gasselt S., Neukum, G., Map-projection-independent crater size-frequency determination in GIS environments—New software tool for ArcGIS. Planetary and Space Science, in press. doi:10.1016/j.pss.2010.03.015.

Kostama, V.P., Kreslavsky, M.A., Head, J.W., 2006. Recent high-latitude icy mantle in the northern plains of Mars: characteristics and ages of emplacement. Geophysical Research Letters 33, L11201. doi:10.1029/2006GL025946.

Kreslavsky, M.A., 2009. Dynamic landscapes at high latitudes on Mars: constraints from populations of small craters. Lunar and Planetary Science Conference XXXX #2311.

Kreslavsky, M.A., Head, J.W., 2002. Mars: nature and evolution of young latitude dependent water–ice-rich mantle. Geophysical Research Letters 29 (1719), 4. doi:10.1029/2002GL015392.

Kreslavsky, M.A., Head, J.W., Maine, A., Gray, H., Asphaug, E., 2010. North-south asymmetry in degradation rates of small impact craters at high latitudes on Mars: implications for recent climate change. Lunar and Planetary Science Conference XXXXI #2560.

Laskar, J., Levrard, B., Mustard, J.F., 2002. Orbital forcing of the Martian polar layered deposits. Nature 419, 375–377. doi:10.1038/nature01066.

Laskar, J., Correia, A.C.M., Gastineau, M., Joutel, F., Levrard, B., Robutel, P., 2004. Long term evolution and chaotic diffusion of the insolation quantities of Mars. Icarus 170 (2), 343–364. doi:10.1016/j.icarus.2004.04.005.

Lefort, A., Russell, P.S., Thomas, N., McEwen, A.S., Dundas, C.M., Kirk, R.L., 2009. Observations of periglacial landforms in Utopia Planitia with the High Resolution Imaging Science Experiment (HiRISE). Journal of Geophysical Research 114, E04005. doi:10.1029/2008JE003264.

Lefort, A., Russell, P.S., Thomas, N., 2010. Scalloped terrains in the Peneus and Amphitrites Paterae region of Mars as observed by HiRISE. Icarus 205, 259–268. doi:10.1016/j.icarus.2009.06.005.

Levrard, B., Forget, F., Montmessin, F., Laskar, J., 2004. Recent ice-rich deposits formed at high latitudes on Mars by sublimation of unstable equatorial ice during low obliquity. Nature 431, 1072–1075. doi:10.1038/nature03055.

Maine, A., Kreslavsky, M.A., Orloff, T.C., Asphaug, E., Gray, H., 2010. Degradation of small crater in the high latitudes of Mars. Lunar and Planetary Science Conference XXXXI #1556.

Malin, M.C., Edgett, K.S., 2001. Mars Global Surveyor Mars Orbiter Camera: interplanetary cruise through primary mission. Journal of Geophysical Research 106, 23429–23570. doi:10.1029/2000JE001455.

Malin, M.C., Edgett, K.S., Posiolova, L.V., McColley, S.M., Dobrea, E.Z.N., 2006. Present-day impact cratering rate and contemporary gully activity on Mars. Science 314, 1573–1577. doi:10.1126/science.1135156.

Malin, M.C., Bell, J.F., Cantor, B.a., Caplinger, M.a., Calvin, W.M., Clancy, R.T., Edgett, K.S., Edwards, L., Haberle, R.M., James, P.B., Lee, S.W., Ravine, M.A., Thomas, P.C., Wolff, M.J., 2007. Context Camera Inestigation on board the Mars Reconnaissance Orbiter. Journal of Geophysical Research 112 (E5), 1–25. doi:10.1029/2006JE002808.

Mangold, N., 2005. High latitude patterned grounds on Mars: classification, distribution and climate control. Icarus 174, 336–359. doi:10.1016/j.icarus.2004.07.030.

Marchant, D.R., Head, J.W., 2007. Antarctic Dry Valleys: microclimate zonation, variable geomorphic processes, and implications for assessing climate change on Mars. Icarus 192 (1), 187–222. doi:10.1016/j.icarus.2007.06.018.

McEwen, A.S., Bierhaus, E.B., 2006. The importance of secondary cratering to age constraints on planetary surfaces. Annuual Review of Earth and Planetary Sciences 34, 540–567.

McEwen, A.S., Eliason, E.M., Bergstrom, J.W., Bridges, N.T., Hansen, C.J., Delamere, W.A., Grant, J.A., Gulick, V.C., Herkenhoff, K.E., Keszthelyi, L., Kirk, R.L., Mellon, M.T., Squyres, S.W., Thomas, N., Weitz, C.M., 2007. Mars Reconnaissance Orbiter's High Resolution Imaging Science Experiment (HiRISE). Journal of Geophysical Research 112 (E5), 1–40. doi:10.1029/2005JE002605.

Mellon, M.T., Jakosky, B.M., 1995. The distribution and behavior of Martian ground ice during past and present epochs. Journal of Geophysical Research 100 (E6), 11781–11799. doi:10.1029/95JE01027.

Mellon, M.T., Feldman, W.C., Prettyman, T.H., 2004. The presence and stability of ground ice in the southern hemisphere of Mars. Icarus 169, 324–340. doi:10.1016/j.icarus.2003.10.022.

Mellon, M.T., Boynton, W.V., Feldman, W.C., Arvidson, R.E., Titus, T.N., Bandfield, J.L., Putzig, N.E., Sizemore, H.G., 2008. A prelanding assessment of the ice table depth and ground ice characteristics in Martian permafrost at the Phoenix landing site. Journal of Geophysical Research 113, E00A25. doi:10.1029/2007JE003067.

Melosh, H.J., 1989. Impact Cratering. A Geologic Process. Oxford Monographs on Geology and Geophysics, New York vol. 11, p. 253.

Michael, G.G., Neukum, G., 2010. Planetary surface dating from crater size-frequency distribution measurements: partial resurfacing events and statistical age uncertainty. Earth and Planetary Science Letters 294, 223–229. doi:10.1016/j.epsl.2009.12.041.

Milliken, R.E., Mustard, J.F.., 2003. Erosional morphologies and characteristics of latitude dependent surface mantles on Mars, in: Sixth International Conference on Mars. Abstract #3240.

Mischna, M.A., Richardson, M.I., Wilson, R.J., McCleese, D.J., 2003. On the orbital forcing of martian water and CO_2 cycles: a general circulation model study with simplified volatile schemes. Journal of Geophysical Research, Planets 108, 5062. doi:10.1029/2003JE002051.

Morgenstern, A., Hauber, E., Reiss, D., van Gasselt, S., Grosse, G., Schirrmeister, L., 2007. Deposition and degradation of a volatile-rich layer in Utopia Planitia, and implications for climate history on Mars. Journal of Geophysical Research 112, E06010. doi:10.1029/2006JE002869.

Mustard, J.F., Cooper, C.D., Rifkin, M.K., 2001. Evidence for recent climate change on Mars from the identification of youthful near-surface ground ice. Nature 412, 411–414. doi:10.1038/35086515.

Neukum, G., Ivanov, B.A., Hartmann, W.K., 2001. Cratering records in the inner solar system in relation to the lunar reference system. Space Science Reviews 96 (55–86), 2001.

Plescia, J.B., 2003. Amphitrites-Peneus Paterae/Malea Planum geology. Lunar and Planetary Science XXXIV Abstract, vol. 1478.

Plescia, J.B., 2004. Morphometric properties of martian volcanoes. Journal of Geophysical Research 109, E03003. doi:10.1029/2002JE002031.

Schon, S.C., Head, J.W., Milliken, R.E., 2009. A recent ice age on Mars: evidence for climate oscillations from regional layering in mid-latitude mantling deposits. Geophysical Research Letters 36, L15202. doi:10.1029/2009GL038554.

Schorghofer, N., 2007. Dynamics of ice ages on Mars. Nature 449, 192. doi:10.1038/nature06082.

Schorghofer, N., Aharonson, O., 2005. Stability and exchange of subsurface ice on Mars. Journal of Geophysical Research 110, E05003. doi:10.1029/2004JE00235.

Siili, T., Haberle, R.M., Murphy, J.R., Savijärvi, H., 1999. Modelling of the combined late-winter ice cap edge and slope winds in Mars' Hellas and Argyre regions. Planetary and Space Science 47, 951–970.

Soare, R.J., Kargel, J.S., Osinski, G.R., Costard, F., 2007. Thermokarst processes and the origin of crater-rim gullies in Utopia and western Elysium Planitia. Icarus 191, 95–112. doi:10.1016/j.icarus.2007.04.018.

Strom, R.G., Croft, S.K., Barlow, N.G., 1992. The Martian Impact Cratering Record. In: Kieffer, H.H., et al. (Eds.), Mars, 1992. University of Arizona Press, Tucson, AZ. doi:10.1016/S0032-0633(99)00016-1, pp. 383–423.

Tanaka, K.L., Leonard, G.J., 1995. Geology and landscape evolution of the Hellas region of Mars. Journal of Geophysical Research 100 (E3), 5407–5432.

Tanaka, K.L., Kargel, J.S., MacKinnon, D.J., Hare, T.M., Hoffman, N., 2002. Catastrophic erosion of Hellas basin rim on Mars induced by magmatic intrusion into volatile rich rocks. Geophysical Research Letters 29 (8), 1195. doi:10.1029/2001GL013885.

Ulrich, M., Morgenstern, A., Günther, F., Reiss, D., Bauch, K.E., Hauber, E., Rössler, S., Schirrmeister, L., 2010. Thermokarst in Siberian ice-rich permafrost: comparison to asymmetric scalloped depressions on Mars. Journal of Geophysical Research 115, E10009. doi:10.1029/2010JE00364.

Werner, S.C., Ivanov, B.A., Neukum, G., 2009. Theoretical analysis of secondary cratering on Mars and an image-based study of the Cerberus Plains. Icarus 200, 406–417. doi:10.1016/j.icarus.2008.10.011.

Williams, D.A., Greeley, R., Werner, S.C., Michael, G., Crown, D.A., Neukum, G., Raitala, J., 2008. Tyrrhena Patera: geologic history derived from Mars Express HRSC. Journal of Geophysical Research 113, E11005. doi:10.1029/2008JE003104.

Williams, D.A., Greeley, R., Fergason, R.L., Kuzmin, R., McCord, T.B., Combe, J.P., Head, J.W., Xiao, L., Manfredi, L., Pouler, F., Piner, P., Baratoux, D., Plaut, J.J., Raitala, J., Neukum, G., 2009. The Circum-Hellas Volcanic Province: overview. Planetary and Space Science 57 (2009), 895–916. doi:10.1016/j.pss.2008.08.010.

Williams, D.A., Greeley, R., Manfredi, L., Fergason, R.L., Combe, J.P., Poulet, F., Pinet, P., Rosemberg, C., Clenet, H., McCord, T.B., Raitala, J., Neukum, G., the HRSC Co-Investigator Team, 2010. Surface-compositional properties of the Malea Planum region of the Circum-Hellas Volcanic Province. Mars Earth and Planetary Science Letters 294 (3–4), 451–465. doi:10.1016/j.epsl.2009.11.019.

Zanetti, M., Hiesinger, H., Reiss, D., Hauber, E., Neukum, G., 2010. Distribution and evolution of scalloped terrain in the southern hemisphere, Mars. Icarus 206, 691–706. doi:10.1016/j.icarus.2009.09.010.